Electronic Supplementary Material (ESI) for Journal of Materials Chemistry A.

Supporting Information

Polyaniline nanofiber array supported ultrathin polyamide membrane for solar-driven volatile organic compounds removal

Xian Wei[a], Yubing Peng[a], Wangxi Fang[b], Zhenyu Hu[c,d], Wenwei Li[c,d], Shenxiang Zhang*[a], Jian Jin*[a]

[a]College of Chemistry, Chemical Engineering and Materials Science; Collaborative Innovation Center of Suzhou Nano Science and Technology; Suzhou Key Laboratory of Macromolecular Design and Precision Synthesis, Soochow University, Suzhou, 215123, China

[b]i-Lab, Suzhou Institute of Nano-Tech and Nano-Bionics, Chinese Academy of Sciences, Suzhou, 215123, China

[c]CAS Key Laboratory of Urban Pollutant Conversion, Department of Applied Chemistry, University of Science & Technology of China, Hefei 230026, China

[d]USTC-CityU Joint Advanced Research Center, Suzhou 215123, China

Supporting Figures

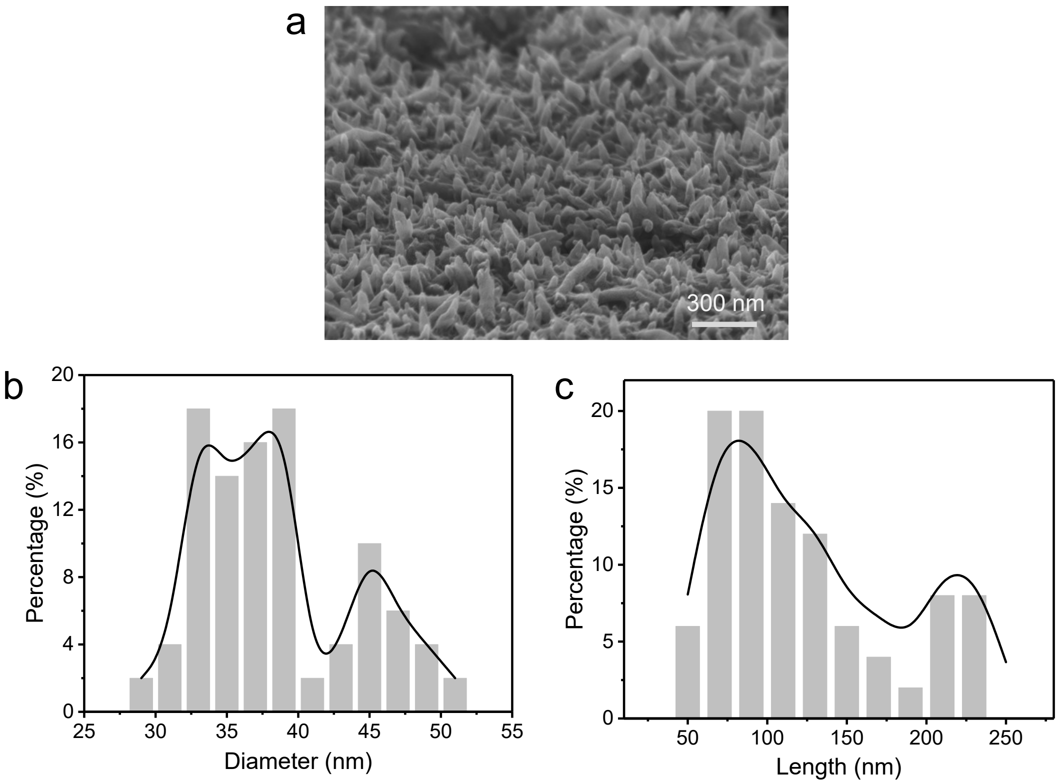

Fig. S1 a) PANI-m SEM image taken at a 45° tilt. b) Diameter and c) length distribution as measured from the SEM image.

Fig. S1a shows the PANI-m SEM image taken at a 45° tilt from a field emission scanning electron microscopy (Hitachi S8230). We measured the diameter and length of the nanofibers respectively. The diameter of PANI fibers was 30-50 nm and the length was 50-250 nm as statistically obtained from the SEM image.

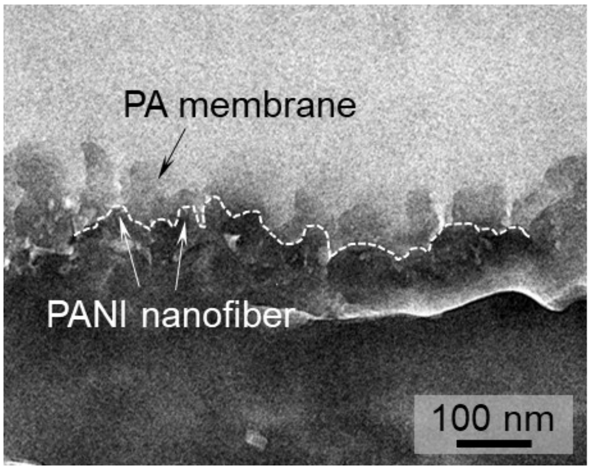

Fig. S2 Cross-section TEM images of the PANI-PA-8.

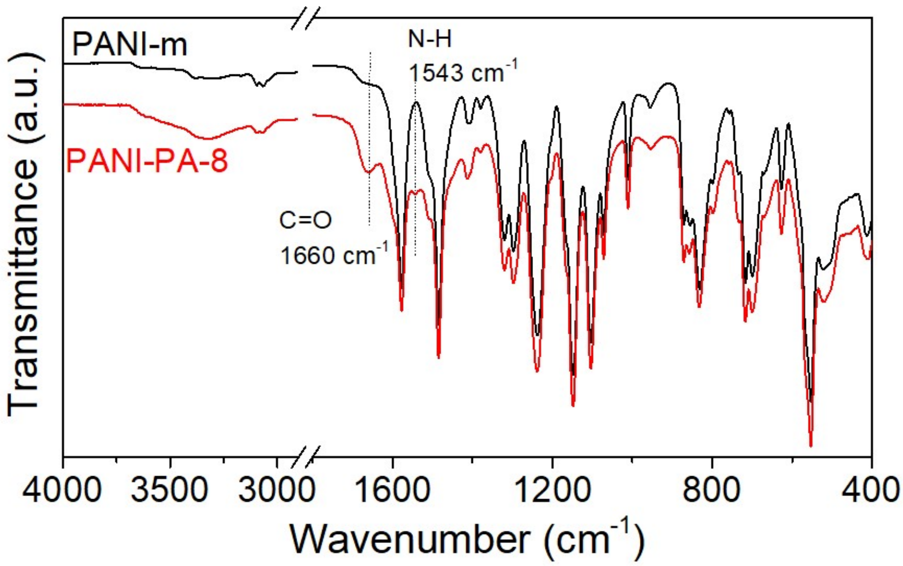

Fig. S3 FTIR spectra of the PANI-m and PANI-PA-8.

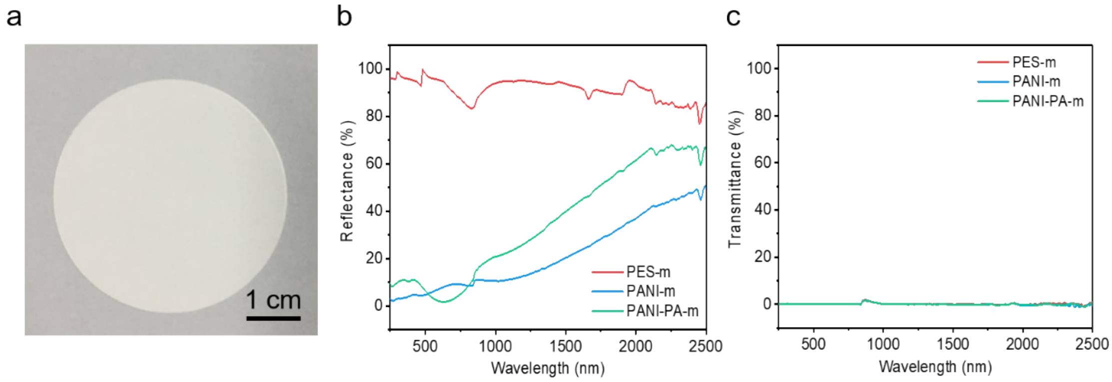

Fig. S4 a) Photograph of the PES-m. b) Light reflectance and c) light transmittance spectra of different membranes at the wavelength from 250 to 2,500 nm.

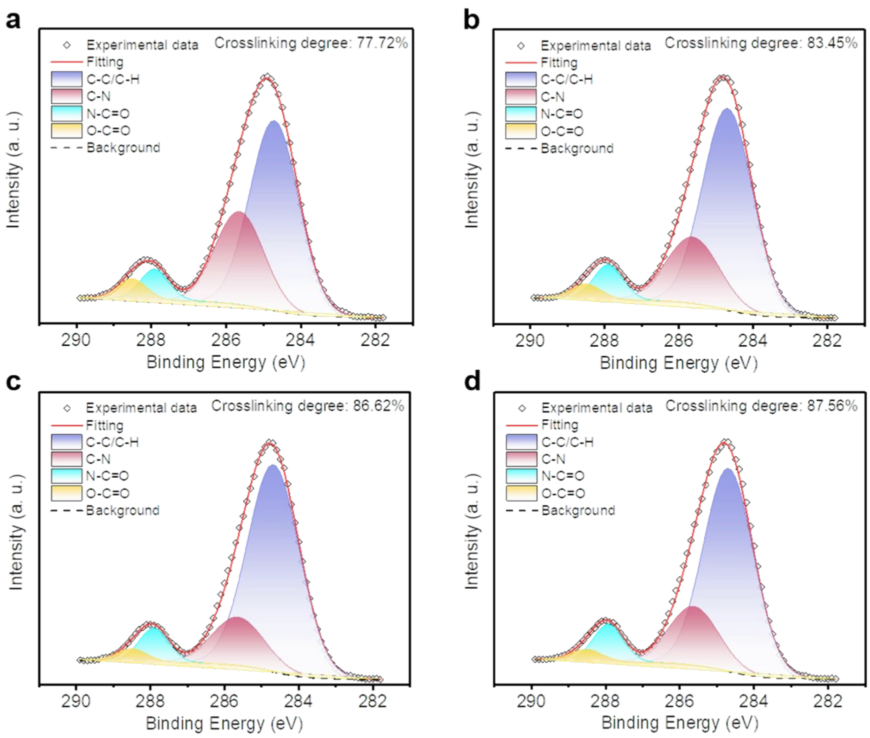

Fig. S5 C 1s XPS spectra of a) PANI-PA-1, b) PANI-PA-2, c) PANI-PA-4 and d) PANI-PA-8.

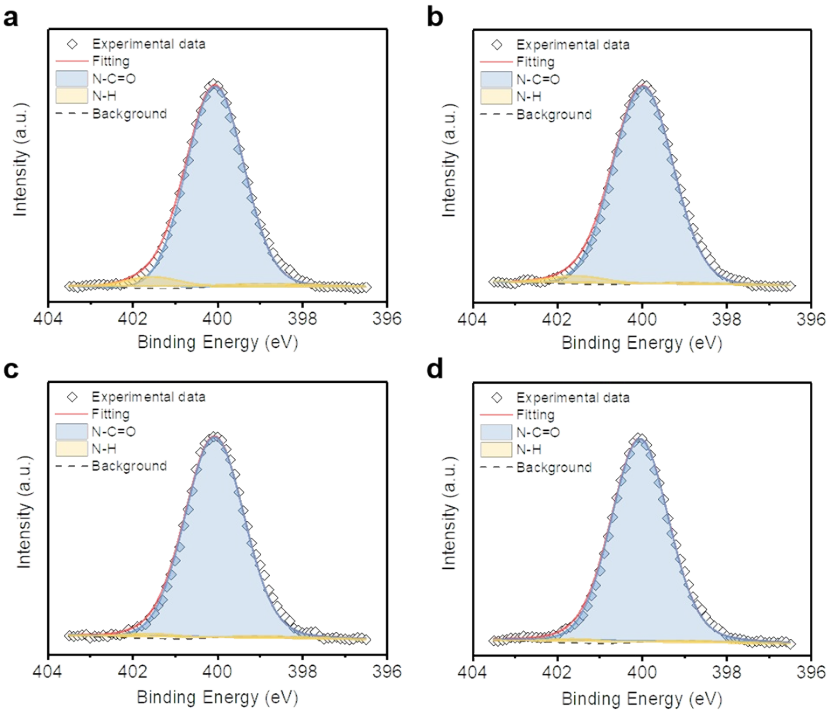

Fig. S6 N 1s XPS spectra of a) PANI-PA-1, b) PANI-PA-2, c) PANI-PA-4 and d) PANI-PA-8.

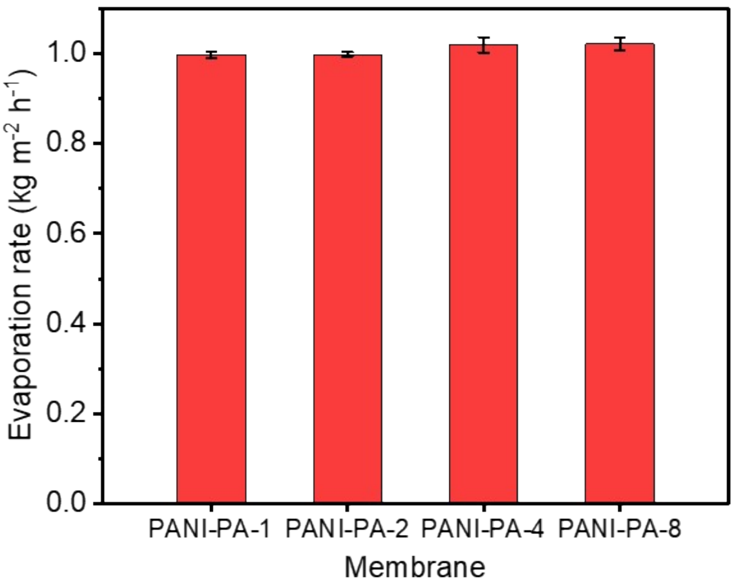

Fig. S7 Water evaporation rates of the PANI-PA-m under 1 sun irradiation.

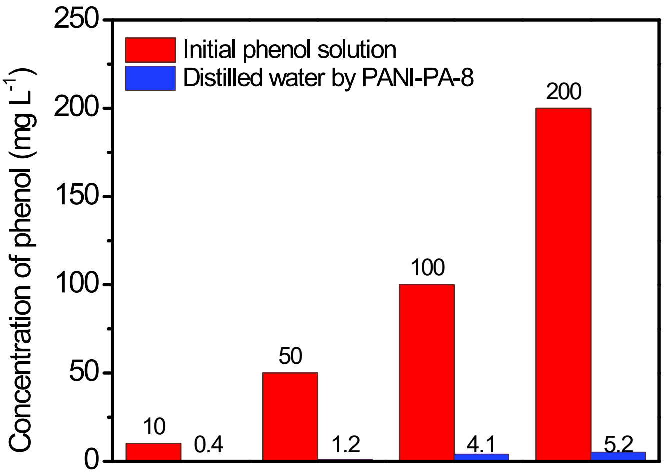

Fig. S8 Phenol concentration in initial aqueous solution and distilled water by the PANI-PA-8 under 1 sun irradiation.

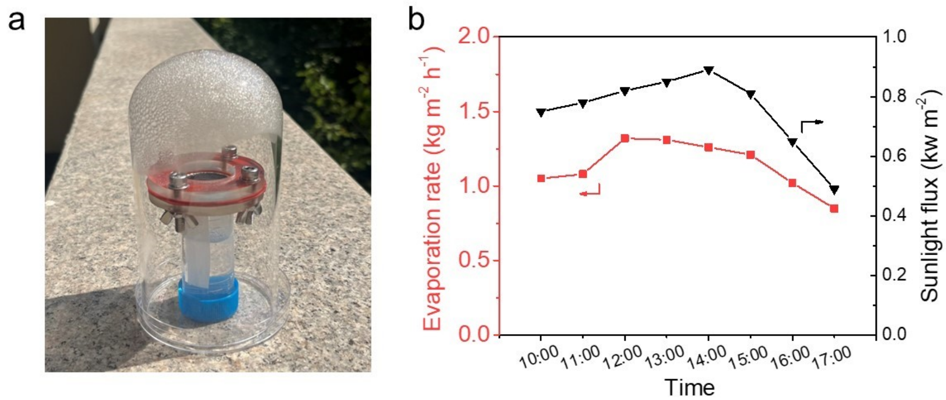

Fig. S9 a) The picture of outdoor solar-driven VOCs removal device. b) Water evaporation rate and sunlight flux during outdoor solar-driven VOCs experiment.

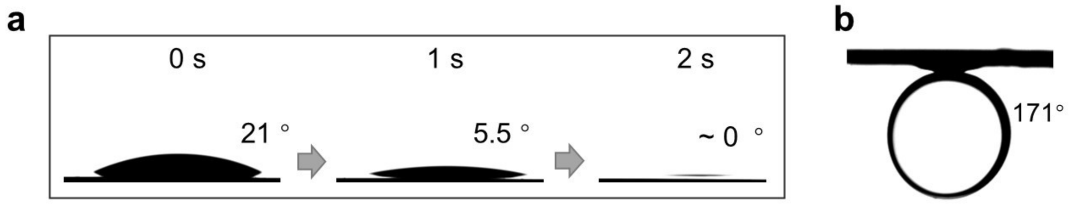

Fig. S10 a) Time-dependent water contact angle of a water droplet and b) underwater oil contact angle of an isooctane droplet on PANI nanofiber arrays.

Membrane pore size characterization

The pore size distribution and molecular weight cutoff (MWCO) of the PANI-PA-m were studied by the rejection rate of a series of neutral organic molecules, including glycerol (92 Da), glucose (180 Da), sucrose (342 Da) and raffinose (504 D a). The feed concentration of each species solution was 200 mg L^{-1} and the applied pressure was 4 bar. The value of MWCO is defined as the molecular weight of the neutral molecule at which the rejection equals 90%. The pore size distribution of the membrane is derived from stokes radius and probability density function of neutral organic molecules. The stokes radius (r_p) is related to the molecular weight of these neutral organic molecules as described in Eq 1:[1]

$$\ln\left(r_p\right) = -1.4962 + 0.4654 \ln\left(MW\right) \tag{1}$$

Where MW is the molecular weight of each organic solute.

Based on the stokes radius of these molecules, the pore size distribution function can be obtained by Eq 2:[1]

$$\frac{dR\left(r_p\right)}{dr_p} = \frac{1}{r_p \ln \sigma_p \sqrt{2\pi}} exp\left[-\frac{\left(\ln r_p - \ln \mu_p\right)^2}{2\left(\ln \sigma_p\right)^2} \right] \tag{2}$$

Where μ_p represents the mean effective pore radius, σ_p represents the geometric standard deviation of probability density function, determined at a ratio of r_p at rejection rate equals 84.13% over that at 50%.

Table S1. Surface chemical components of the PANI-PA-m.

Membrane	C (%)	Surface chemical species from C1s			N (%)	Surface chemical species from N1s			O (%)	Crosslinking degree (%)
		B.E. (eV)	Species	Content (%)		B.E. (eV)	Species	Content (%)		
PANI-PA-1	73.32	284.7	C-C/C-H	44.18	13.83	400	O=C-N	13.05	12.85	77.72
		285.6	C-N	21.67		401.5	N-H	**0.78**		
		287.9	O=C-N	4.51						
		288.5	O=C-O	**2.96**						
PANI-PA-2	73.57	284.7	C-C/C-H	49.42	13.66	400	O=C-N	13.11	12.77	83.45
		285.6	C-N	17.13		401.5	N-H	**0.55**		
		287.9	O=C-N	4.97						
		288.5	O=C-O	**2.05**						
PANI-PA-4	73.80	284.7	C-C/C-H	54.37	13.92	400	O=C-N	13.59	12.28	86.62
		285.6	C-N	12.69		401.5	N-H	**0.33**		
		287.9	O=C-N	4.97						
		288.5	O=C-O	**1.77**						
PANI-PA-8	73.02	284.7	C-C/C-H	50.95	14.02	400	O=C-N	13.73	12.96	87.56
		285.6	C-N	14.81		401.5	N-H	**0.29**		
		287.9	O=C-N	5.60						
		288.5	O=C-O	**1.66**						

The crosslinking degree was calculated by the following equation:[2]

$$\text{Crosslinking Degree} = \frac{amide\ links}{potential\ amide\ links} = \frac{N - AG}{N + CG}$$

Where N, AG, and CG represent the content of nitrogen, amine groups, and carboxylic groups respectively in the active layer.

Tab. S2. Phenol removal performance by using solar-driven process.

Material	Mechanism	Initial concentration (mg L^{-1})	Light density (kw m^{-2})	Water evaporation rate (kg m^{-2} h^{-1})	Removal rate	Reference
Persulfate	Photo-Fenton reaction	1	5	2.8	~ 50 %	3
Polypyrrole	Solution-diffusion separation	5	1	1.12	90 %	4
P25-coated Flammulina	photocatalytic degradation	5	1	~ 1.0	78 %	5
Zr–Fc MOF	Photo-Fenton reaction	10	1	1.53	~ 95 %	6
TiO_{2-x}	photocatalytic degradation	10	1	1.05	95 %	7
Peroxymonosulfate	Photo-Fenton reaction	10	1	1.14	96 %	8
$CuFeMnO_4$	Photo-Fenton reaction	100	1	1.78	87 %	9
Alginate	Solution-diffusion separation	100	1	1.4	99 %	10
Polyamide	Molecular sieving separation	200	1	1.02	98 %	This work

Supporting References

1. L. Zhang, R. Zhang, M. Ji, Y. Lu, Y. Zhu, J. Jin, *J. Membr. Sci.,* 2021, **636,** 119478.

2. O. Coronell, B. J. Mariñas, D. G. Cahill, *Environ. Sci. Technol.,* 2011, **45,** 4513-4520.

3. R. Chen, T. Zhang, J. Kim, H. Peng, M. Ye, C.-H. Huang, *Environ. Sci. Technol.,* 2021, **55,** 6248-6256.

4. D. Qi, Y. Liu, Y. Liu, Z. Liu, Y. Luo, H. Xu, X. Zhou, J. Zhang, H. Yang, W. Wang, *Adv. Mater.,* 2020, **32,** 2004401.

5. J. Deng, S. Xiao, B. Wang, Q. Li, G. Li, D. Zhang, H. Li, *ACS Appl. Mater. Interfaces,* 2020, **12,** 51537-51545.

6. X. Ma, Z. Deng, Z. Li, D. Chen, X. Wan, X. Wang, X. Peng, *J. Mater. Chem. A,* 2020, **8,** 22728-22735.

7. C. Song, D. Qi, Y. Han, Y. Xu, H. Xu, S. You, W. Wang, C. Wang, Y. Wei, J. Ma, *Environ. Sci. Technol.,* 2020, **54,** 9025-9033.

8. S. Zuo, D. Xia, Z. Guan, F. Yang, S. Cheng, H. Xu, R. Wan, D. Li, M. Liu, *Sep. Purif. Technol.,* 2021, **254,** 117611.

9. L. Shi, Y. Shi, S. Zhuo, C. Zhang, Y. Aldrees, S. Aleid, P. Wang, *Nano Energy,* 2019, **60,** 222-230.

10. P. Zhang, F. Zhao, W. Shi, H. Lu, X. Zhou, Y. Guo, G. Yu, *Adv. Mater.,* 2022, **34,** 2110548.